Atmos. Chem. Phys. Discuss., 8, 11363–11395, 2008
www.atmos-chem-phys-discuss.net/8/11363/2008/

Atmospheric Chemistry and Physics Discussions

Aerosol dynamics simulations on the connection of sulphuric acid and new particle formation

S.-L. Sihto[1], H. Vuollekoski[1], J. Leppä[2], I. Riipinen[1], V.-M. Kerminen[2], H. Korhonen[3], K. E. J. Lehtinen[3,4], M. Boy[1], and M. Kulmala[1]

[1]Univ. of Helsinki, Dept. of Physics, P.O. Box 64, FI-00014 University of Helsinki, Finland
[2]Finnish Meteorological Institute, Climate and Global Change, P.O. Box 503, FI-00101 Helsinki, Finland
[3]University of Kuopio, Department of Physics, P.O. Box 1627, FI-70211 Kuopio, Finland
[4]Finnish Meteorological Institute, Kuopio Unit, P.O. Box 1627, FI-70211 Kuopio, Finland

Received: 11 April 2008 – Accepted: 25 April 2008 – Published: 10 June 2008

Correspondence to: S.-L. Sihto (sanna-liisa.sihto@helsinki.fi)

Published by Copernicus Publications on behalf of the European Geosciences Union.

Abstract

We have performed a series of simulations with an aerosol dynamics box model to study the connection between new particle formation and sulphuric acid concentration. For nucleation either activation mechanism with a linear dependence on the sulphuric acid concentration or ternary H_2O-H_2SO_4-NH_3 nucleation was assumed. We investigated the factors that affect the sulphuric acid dependence during the early stages of particle growth, and tried to find conditions which would yield the linear dependence between the particle number concentration at 3–6 nm and sulphuric acid, as observed in field experiments. The simulations showed that the correlation with sulphuric acid may change during the growth from nucleation size to 3–6 nm size range, the main reason being the size dependent growth rate between 1 and 3 nm. In addition, the assumed size for the nucleated clusters had a crucial impact on the sulphuric acid dependence at 3 nm. The simulations yielded a linear dependence between the particle number concentration at 3 nm and sulphuric acid, when a low saturation vapour pressure for the condensable organic vapour was assumed, or when nucleation took place at ~2 nm instead of ~1 nm. Comparison of results with activation and ternary nucleation showed that ternary nucleation cannot explain the experimentally observed linear or square dependence on sulphuric acid.

1 Introduction

Particle formation from gaseous precursors is an important source of particles in the atmosphere. Events of new particle formation starting with nucleation of tiny clusters and followed by growth to bigger, climatically relevant sizes, have been observed all around the world, from remote locations to polluted urban cities (Kulmala et al., 2004a). Regionally, atmospheric particle formation may give a dominant contribution to the total particle number concentration (Spracklen et al., 2006, Tunved et al., 2006) and affect significantly both cloud condensation nuclei and cloud droplet concentrations

ACPD

8, 11363–11395, 2008

(Kerminen et al., 2005; Laaksonen et al., 2005; Spracklen et al., 2008).

Aerosol particles affect the climate directly by scattering and absorbing radiation, and indirectly by influencing the cloud formation and by modifying the cloud properties. The aerosol indirect effect is one of the most poorly known factors of the climate system (Penner et al., 2006; Rosenfeld, 2006; IPCC, 2007; Baker and Peter, 2008). Besides the uncertainties associated with aerosol-climate interactions, the mechanism of atmospheric nucleation is still unclear. Due to these uncertainties and computational cost of modelling the full aerosol dynamics, most climate models have a very crude representation of aerosol processes. Thus there is a need for detailed understanding of the relevant processes, in order to develop accurate, yet computationally efficient parameterizations applicable to large-scale modeling frameworks.

Field measurements of aerosol particle and sulphuric acid concentrations have shown that atmospheric new particle formation seems to be a function of gaseous sulphuric acid concentration to the power of 1–2 (Weber et al., 1996, 1997; Sihto et al., 2006; Riipinen et al., 2007; Kuang et al., 2008). This dependence is in contrast with the theory of ternary sulphuric acid–water–ammonia nucleation (Napari et al., 2002) which predicts critical cluster sizes of 4–10 molecules, yielding correlation exponents of 4–10 between nucleation rate and sulphuric acid concentration. To explain the observations, nucleation mechanisms known as activation and kinetic nucleation have been proposed (Kulmala et al., 2006), with nucleation rate linearly or squarely dependent on sulphuric acid concentration. The activation type nucleation mechanism has been applied in a global aerosol microphysics model (Spracklen et al., 2006), showing very good agreement with measurements performed at SMEAR II station in Hyytiälä, Finland.

Conventional atmospheric particle number concentration measurements start from particle diameter of 3 nm, while actual nucleation, i.e. formation of stable clusters, happens at smaller sizes, well below 3 nm. Recently there have been advances in measuring sub-3 nm neutral and charged particles in field (Kulmala et al., 2007), which indicate that atmospheric nucleation starts at 1.5–2 nm size range. However, the observed

ACPD
8, 11363–11395, 2008

correlations with sulphuric acid have so far been done with particle concentrations at 3–6 nm (Sihto et al., 2006; Riipinen et al., 2007). From these dependences for 3 nm particles, one would like to extrapolate the similar dependence for nucleated clusters. This is not straightforward, since between the nucleation size and 3 nm, particles are subject to size-dependent aerosol dynamical processes: they grow by condensation of sulphuric acid and/or other vapours, and are lost in coagulation with each other and with background aerosol particles (e.g. McMurry, 1983; Kerminen et al., 2004; McMurry et al., 2005). Therefore the dependence of particle formation on sulphuric acid concentration may change as particles grow to larger sizes.

Aerosol dynamics modelling offers a tool to investigate the factors that influence the connection between sulphuric acid and new particle formation during the early stages of particle growth. We have performed a series of simulations with a sectional aerosol dynamics box model UHMA (University of Helsinki Multicomponent Aerosol model) to study this connection in detail. In particular, we tried to find conditions which would yield the observed linear dependence between the particle number concentration and sulphuric acid, and investigated how the dependence on sulphuric acid concentration changes as particles grow from nucleation size to larger sizes.

2 Modelling approach

2.1 UHMA model

The aerosol dynamics model UHMA (University of Helsinki Multicomponent Aerosol model, Korhonen et al., 2004) is a sectional box model designed to study new particle formation and growth. It has all the basic aerosol microphysical mechanisms for clear sky conditions implemented: nucleation, condensation, coagulation and dry deposition. In previous studies UHMA has been extended to include cloud processing (Korhonen et al., 2005), it has been applied in a Lagrangian trajectory study (Komppula et al., 2006), and it has been implemented as a part of the 1-D columnar model MALTE (Boy

et al., 2006). For this study, the basic box-model version of UHMA is sufficient. Here we describe briefly the features of the model relevant to this study; for more details we refer the reader to Korhonen et al. (2004).

In the UHMA model, particles are assumed to consist of sulphuric acid, water, ammonia and an organic model-compound, and to be internally mixed inside a size section. As input for the model, an initial size distribution, ambient meteorological conditions (temperature, relative humidity) and gas concentrations for the condensing vapours must be given. The model then calculates the evolution of the particle size distribution subject to aerosol dynamical processes.

Condensation and coagulation are calculated according to the conventional equations by Fuchs and Sutugin (1971). However, for condensation in the free-molecular regime we apply a modification by Lehtinen and Kulmala (2003). It takes into account the particle diffusion coefficient and diameter of the condensing molecule, when calculating the particle Knudsen number and coagulation coefficient – these are normally assumed negligible compared to the vapour diffusion coefficient and particle diameter. The modified condensation theory approaches the free-molecular coagulation theory in the limit of free molecular particles. The correction increases the free-molecular regime condensation flux compared to the traditional Fuchs-Sutugin expression, and is significant for particle sizes d_p<10 nm.

In these simulations, we apply two condensing vapours: sulphuric acid and an organic model-compound, which represents the oxidation products of biogenic volatile organic compounds (BVOCs, e.g. monoterpenes) emitted by the vegetation. The semi-volatile oxidated organic compounds are expected to contribute a significant fraction of the particle growth in Boreal forest (Kulmala et al., 2004b; Boy et al., 2005; Hirsikko et al., 2005).

Sulphuric acid production rate is calculated as a chemical reaction rate between SO_2 and OH, while the OH concentration is dependent on the solar zenith angle. This results in a sinusoidal profile for sulphuric acid concentration with a maximum value around noon. The saturation vapour concentration of sulphuric acid is assumed to be

ACPD
8, 11363–11395, 2008

negligible, i.e. it condenses with the maximum flux without Kelvin effect (c_{sat}=0).

The condensation of a water-soluble, semi-volatile organic vapor is calculated with the nano-Köhler mechanism (Kulmala et al., 2004c), which takes into account the Kelvin effect and the solubility effect (Raoult effect), analogously to the traditional Köhler-theory. However, instead of describing the equilibrium of μm-sized cloud droplets with water vapour, nano-Köhler theory considers nm-sized clusters, consisting of ammonium bisulphate, organic compound and water, in equilibrium with a water-soluble organic vapour. The equilibrium of the organic vapour over a spherical particle is governed by the two Köhler-type equations:

$$p_{eq,org} = p_{s,org}\gamma_{org}\exp\left(\frac{4\sigma m_{org}}{RT\rho_{org}d_p}\right) \quad , \tag{1}$$

$$p_{eq,w} = p_{s,w}\gamma_{w}\exp\left(\frac{4\sigma m_{w}}{RT\rho_{w}d_p}\right) \quad . \tag{2}$$

The first equation refers to organic vapour (org) and second to water vapour (w). Here $p_{s,org}$ ($p_{s,w}$) is the saturation vapour pressure of pure organic vapour (water) over flat surface, γ_{org} (γ_w) the activity coefficient of the organic compound (water), d_p the particle diameter, T temperature, k_B Boltzmann's constant, σ surface tension of the droplet, m_{org} (m_w) molecular mass and ρ_{org} (ρ_w) density of the organic compound (water). The two equations must be solved simultaneously. For estimating the activity coefficients and surface tensions, the solution is assumed to behave as pseudobinary, consisting of an organic compound and ammonium bisulphate with the associated water. The volatility of the organic vapor can be varied by changing its saturation vapour pressure $p_{s,org}$, or saturation vapour concentration (c_{sat}) which we will use here.

For water vapour and ammonia condensation is not calculated dynamically, but through a parameterization for the equilibrium uptake of water and ammonia that depends on the particle composition.

ACPD
8, 11363–11395, 2008

For nucleation, several mechanisms can be utilized: binary H_2O-H_2SO_4 (Vehkamäki et al., 2002) and ternary H_2O-H_2SO_4-NH_3 (Napari et al, 2002) nucleation, kinetic nucleation of ammonium bisulphate molecules, and activation nucleation (Kulmala et al., 2006). Here we made simulations with activation nucleation and ternary H_2O-H_2SO_4-NH_3 nucleation. According to the activation nucleation mechanism, the nucleation rate is directly proportional to sulphuric acid concentration:

$$J_{act} = A\,[H_2SO_4]\,, \tag{3}$$

where A is an empirical nucleation coefficient. The idea of the activation nucleation mechanism is based on the observed linear dependence between new particle formation and sulphuric acid concentration (Kulmala et al., 2006; Sihto et al., 2006). For the coefficient A we used the value determined for the QUEST II campaign in Hyytiälä, Finland, A=10^{-6} s^{-1} (Sihto et al., 2006).

For the activation nucleation mechanism, we have to presume an initial size and composition for the nucleated particles. As a base case, the size of nucleated particles was taken to be 1 nm dry diameter and particles were assumed to consist only of sulphuric acid. The assumption of pure sulphuric acid clusters is somewhat unrealistic, because in reality the nucleated clusters most probably consist of several different molecules, e.g. sulphuric acid, ammonia, water and possibly other molecules. However, sensitivity tests showed that the initial particle composition didn't have a significant effect on model results. When the nucleated particles are created in the model, their composition starts to change immediately: particles take up water and ammonia, and condensation of H_2SO_4 and organics further change the particle dry composition, which after some timesteps makes the initial particle composition irrelevant.

Particle dry deposition is calculated according to a parameterisation that is based on particle flux measurements in Hyytiälä, a Boreal forest site (Rannik et al., 2003).

ACPD
8, 11363–11395, 2008

2.2 Simulation parameters

The simulation parameters were chosen to represent typical conditions of a Boreal forest site in Hyytiälä, Finland. The sulphuric acid concentration had a sinusoidal profile with a maximum of 5–7·10^6 cm^{-3}. The sulphuric acid production rate was same in all simulations, but due to different growth rates, the condensation sink differed between the simulation cases, which resulted in slightly different maximum values for sulphuric acid concentration. For the condensable organic vapour we used a constant concentration of 10^7 cm^{-3} in order to keep the modelling setup simple. The volatility of the organic vapor was varied by changing its saturation vapour concentration. The simulations were performed by the fixed sections hybrid approach (for details of the method see Korhonen et al., 2004) with 50 size sections between 0.65 nm and 1 μm (diameter).

To illustrate the connection of sulphuric acid and new particle formation, we present the results for four basic cases which describe the essential features of the system (see Table 1). In the simulations we varied the nucleation mechanism and the saturation concentration of the condensable organic vapour. In addition, the effect of the different nucleated cluster sizes (d_{nuc}=1–2 nm) was investigated. Altogether, including sensitivity analyses, around 500 simulation runs were performed.

2.3 Analysis of correlations

Field measurements have indicated that new particle formation is related to the sulphuric acid concentration to the power from 1 to 2 (Weber et al., 1996, 1997; Sihto et al., 2006; Riipinen et al., 2007). The previous studies have considered the number concentration of 3–6 nm particles (N_{3-6}) and the formation rate of 3 nm particles (J_3), due to the fact that particle measurements start at 3 nm. Here we consider the same quantities, in order to compare the simulation results with the measurements.

The studied correlations can be expressed mathematically in the form:

$$N_{3-6}(t) \sim [H_2SO_4]^{n_{N_{3-6}}} (t - \Delta t_{N_{3-6}})$$
$$J_3(t) \sim [H_2SO_4]^{n_{J_3}} (t - \Delta t_{J_3}) \quad (4)$$

ACPD
8, 11363–11395, 2008

In words this means that N_{3-6} (J_3) follows the H_2SO_4 concentration to the power of n_{N3-6} (n_{J3}) with a time delay Δt_{N3-6} (Δt_{J3}). Because nucleation and sulphuric acid are directly related, the time delay arises from the time required for growth from nucleation size (1–2 nm) to 3 nm.

The correlations can be easily investigated by plotting N_{3-6} or J_3 versus [H_2SO_4] in logarithmic scale. In such scatter plots power relationships appear as straight lines with slope of the line giving the exponent of correlation:

$$\begin{aligned} \ln\left(N_{3-6}\right) &\sim n_{N_{3-6}} \ln\left([H_2SO_4]\right)(t - \Delta t_{N_{3-6}}) \\ \ln\left(J_3\right) &\sim n_{J_3} \ln\left([H_2SO_4]\right)(t - \Delta t_{J_3}) \quad . \end{aligned} \tag{5}$$

From data analysis from a Finnish and a German station Riipinen et al. (2007) reported values n_{N3-6}=1–2 and n_{J3}=1–3 for the exponents and Δt_{N3-6}=0.8–4.5 h and Δt_{J3}=0.5–4.2 h for the time delays. Moreover, it was observed that $n_{N3-6} \leq n_{J3}$ and that $n_{N3-6} \leq n_{\mathrm{nuc}}$, where n_{nuc} is the exponent of nucleation. The time delays behaved as $\Delta t_{J3} \leq \Delta t_{N3-6}$, i.e. the rise in N_{3-6} is always preceded by the rise in J_3.

The purpose of this study was to investigate how the correlation with sulphuric acid changes during the growth from nucleation size (1–2 nm) to sizes of 3–6 nm. If we have a linear dependence with sulphuric acid in nucleation rate J_{nuc} (as according to activation nucleation, Eq. 3), what is the relationship between J_3 and [H_2SO_4] or N_{3-6} and [H_2SO_4]? If the relationship changes, what are the reasons for the change?

From the simulation data, N_{3-6} was calculated simply as a sum of concentrations of the size bins in the range 3–6 nm. Formation rate of 3 nm particles (J_3) was calculated as follows:

$$J_3 = \frac{N_3}{\Delta d_p} GR_3 \quad , \tag{6}$$

where N_3 is particle number concentration in a size bin of width Δd_p around particle diameter 3 nm and GR_3 is the growth rate of 3 nm particles.

ACPD
8, 11363–11395, 2008

The particle growth rate can be calculated from the simulated volume change rate of particles:

$$\frac{dv}{dt} = \frac{d}{dt}\left(\frac{4}{3}\pi d_p^3\right) = 4\pi d_p^2 \frac{dd_p}{dt} \quad .$$

By denoting $dd_p/dt = GR$, we can solve the growth rate:

$$GR(d_p) = \frac{dd_p}{dt} = \frac{1}{4\pi d_p^2}\frac{dv(d_p)}{dt} \quad . \tag{7}$$

The volume change rate $dv(d_p)/dt$ due to condensation or evaporation is obtained as output from the simulation for every size section. Using Eq. (6) we can calculate the particle growth rate as a function of particle size.

3 Results and discussion

The simulation results are presented as four cases, for which the key parameters are listed in Table 1. Case 1 is considered a base case with activation nucleation (Eq. 3) as a nucleation mechanism and organic vapour treated as semi-volatile having a saturation vapour concentration $c_{sat,org}$=10^6 cm^{-3}.

Figure 1 shows the evolution of particle size distribution for the new particle formation events of different simulation cases. As an input, a background aerosol distribution corresponding to a typical distribution at the Boreal forest site in Hyytiälä, Finland, was given. With the specified gas concentrations (see Fig. 2), evolution of aerosol size distribution was simulated according to aerosol dynamical processes, with no further constraints on background aerosol. Nucleation happens around noon, following the sulphuric acid concentration profile. Nucleated particles grow by condensation of H_2SO_4 and an organic vapour, resulting in a growing nucleation mode i.e. a new particle formation event. Also background particle distribution grows by condensation of H_2SO_4 and organic vapour.

ACPD
8, 11363–11395, 2008

From Fig. 1 some important differences between the simulation cases can be observed: With activation nucleation (cases 1 and 2) 1–2 nm sized particles are formed throughout the whole one day simulation, whereas with ternary nucleation (cases 3 and 4) particles are produced for a shorter time but with a greater intensity. This results in a more intense nucleation event with ternary nucleation. The effect of the organic vapour saturation concentration shows in the growth of freshly nucleated particles, especially below particle size of 3 nm. With low organic vapour saturation concentration ($c_{sat,org}$=0 cm^{-3}, cases 2 and 4) freshly nucleated particles grow at a significantly bigger rate than with higher saturation concentration ($c_{sat,org}$=10^6 cm^{-3}, cases 1 and 3). This changes the shape of the particle formation event and makes it broader for the cases with low $c_{sat,org}$. Also, particle formation event becomes more intense, when bigger growth rate makes greater fraction of nucleated particles to survive to bigger sizes before coagulating with background particles.

In the following we investigate the correlations of formation rate of 3 nm particles (J_3) and 3–6 nm particle number concentration (N_{3-6}) with sulphuric acid. The profiles of simulated J_3 and N_{3-6} as a function of time, together with the condensable gas concentrations which were given as input for the simulation, are shown in Fig. 2 for all simulation cases. First we present the model results for the case 1, and then compare it with other simulation cases.

3.1 General correlation of J_{nuc}, J_3, and N_{3-6} with sulphuric acid concentration

In this study we are interested in the relationship between sulphuric acid concentration and freshly nucleated particles, and specifically in how the relationship changes during particle growth from nucleation size to 3-6 nm size range. Figure 3a presents the sulphuric acid concentration and number concentration of 3-6 nm particles (N_{3-6}) for the simulation case 1. Sulphuric acid has a sinusoidal profile, and rise in [H_2SO_4] is followed by rise in N_{3-6} after some time delay that is required for growth from ~1 nm to 3 nm. This time delay is a key parameter in interpreting the relationship between

ACPD
8, 11363–11395, 2008

$[H_2SO_4]$ and N_{3-6}.

The correlation between N_{3-6} and $[H_2SO_4]$ can be seen more clearly by plotting N_{3-6} against $[H_2SO_4]$ (Fig. 3c). Plotted in log-log scale, the power relationships appear as straight lines with slope of the line giving the exponent of correlation. The figure shows a clear correlation between the quantities, but with a different slope in the morning (when $[H_2SO_4]$ is increasing) and in the afternoon (when $[H_2SO_4]$ is decreasing) (see colour code for time of the day). However, by taking into account the time delay between $[H_2SO_4]$ and N_{3-6}, the correlation stays the same for most of the event time. This is demonstrated in Fig. 3d where delaying $[H_2SO_4]$ curve by Δt_{N3-6}=1.5 h makes the two branches of the scatter plot to almost coincide on top of each other. The time delay was determined visually by searching for the value that gives the best correlation between N_{3-6} and $[H_2SO_4]$. Fitting a line to the logarithmic data gives the correlation exponent $n_{N3-6}\approx 2.3$ ($\ln(N_{3-6}) \sim n_{N3-6} \times \ln([H_2SO_4])(t-\Delta t_{N3-6})$). The relationship between N_{3-6} and $[H_2SO_4]$ is also shown in Fig. 3b where $[H_2SO_4]$ values have been delayed by Δt_{N3-6}=1.5 h and raised to the exponent n_{N3-6}=2.3.

The scatter plots of Fig. 3 show that the time delay between $[H_2SO_4]$ and N_{3-6} is of crucial importance when studying the correlation between these quantities. Using improper time delay can lead to misleading or false conclusions. For example, the correlation exponents determined from the data without any time shift (Fig. 3c), would be $n\approx 7.3$ for the rising part and $n\approx 1.2$ for the decreasing part of the curve.

One may question which way of looking at the data is correct: with or without the time shift. We claim that the time delay has to be taken into account. There are several reasons for this: First, with the time delay, there is the same correlation (with the same exponent) between N_{3-6} and $[H_2SO_4]$ during most of the event time (see Fig. 3d). This gives confidence that the correlation is not an artefact. Second, the time delay between N_{3-6} and $[H_2SO_4]$ means that it is the nucleation rate that depends on $[H_2SO_4]$, and not J_3 or N_{3-6}. This is what is expected, and the time delay arises due to the finite growth time from the nucleation size to 3 nm.

It is somewhat surprising that a constant time delay works fairly well for the whole

ACPD
8, 11363–11395, 2008

new particle formation event, even though the particle growth rate is not constant, but changes both as a function of time and particle size (see Sect. 3.2 for more discussion).

Previously Sihto et al. (2006) and Riipinen et al. (2007) have investigated similar correlations in field measurement data. In their study, correlation exponent and time delay (n_{N3-6} and Δt_{N3-6} or n_{J3} and Δt_{J3}) were determined by finding a combination that gave the maximum correlation coefficient between J_3 or N_{3-6} and $[H_2SO_4]^n$. This method worked well with measured data, but not with the simulated data: the simulated J_3, N_{3-6} and $[H_2SO_4]$ were so smooth, that correlation coefficient was close to unity with any choice of exponent and time delay, and therefore the method could not distinguish the best correlation exponent and time delay. Nevertheless, with scatter plots the correlation between J_3 or N_{3-6} and $[H_2SO_4]$ could be investigated easily, and time delays and correlation exponents were straightforward to determine.

3.2 Effect of size-dependent particle growth rate: organic vapour and sulphuric acid

We now present the correlations of simulated J_3 and N_{3-6} with $[H_2SO_4]$ using scatter plots, where the time delay between $[H_2SO_4]$ and J_3 or N_{3-6} was determined visually (as described above for N_{3-6}; see Fig. 3). For simulation case 1, the correlation exponent with $[H_2SO_4]$ was significantly different for nucleation rate at ~1 nm (J_{nuc}) and for formation rate at 3 nm (J_3) (Fig. 4a and b). In addition, the correlation exponent for N_{3-6} was different than for the formation rates (Fig. 4c). With activation as nucleation mechanism, the correlation exponent for J_{nuc} is n_{nuc}=1, but for J_3 the exponent changed to $n_{J3}\approx$3.2 (exponent fitted to the logarithmic data). For N_{3-6} the exponent was slightly smaller than for J_3, $n_{N3-6}\approx$2.3. In the scatter plots the time of day is indicated by colour, showing that correlation changes somewhat, especially for N_{3-6}, during the course of the one-day simulation.

The steeper dependence on sulphuric acid for J_3 than for N_{3-6} ($n_{J3}\geq n_{N3-6}$) is consistent with the measurement data analysis (Riipinen et al., 2007). In addition, J_3 starts to increase before N_{3-6}: the time delay between $[H_2SO_4]$ and J_3 is Δt_{J3}=0.8 h, but between $[H_2SO_4]$ and N_{3-6} the time delay is Δt_{N3-6}=1.5 h. These are explained

by number concentration being an integral quantity of the formation rate.

In field measurement data, J_3 and N_{3-6} are observed to correlate with sulphuric acid concentration to the power of 1–2 (Riipinen et al., 2007). Thus the results of simulation case 1, with correlation exponents close to 3, seem not to correspond the observations very well. Therefore we tried to find parameters that would yield lower correlation exponents for J_3 and N_{3-6}.

The relationship of J_3 and N_{3-6} with sulphuric acid was greatly affected by the growth rate between 1 and 3 nm. In case 1, the growth between 1 and 3 nm was mainly by sulphuric acid, but after 2 nm the organic vapour started to condense gradually according to nano-Köhler mechanism. The growth rate profile between 1 and 12 nm and the contributions of sulphuric acid and organic vapour are presented in Fig. 5. Below ~4 nm, the growth rate due to sulphuric acid increases with decreasing particle size. This results from the molecular enhancement in the condensation flux (Lehtinen and Kulmala, 2003). Combined with the growth rate due to nano-Köhler organics, which increases with particle size at size range 1–4 nm, we get the total growth rate that has a minimum around d_p=2 nm. Besides the size dependence, the growth rate varies also as a function of time, according to the gas concentrations (variability indicated by grey areas in Fig. 5). Since organic vapour concentration is kept constant, only the sulphuric acid part of the growth rate changes during the simulation.

The minimum in growth rate causes a bottleneck effect that retards the increase of J_3 and N_{3-6} compared to nucleation rate J_{nuc}. This may be the reason why in case 1 the relationship with sulphuric acid for J_3 and N_{3-6} differs clearly from that for J_{nuc}.

We made a set of simulations, in which the saturation concentration of organic vapour ($c_{\mathrm{sat,org}}$) was lowered from $10^6\,\mathrm{cm}^{-3}$ (case 1) to $0\,\mathrm{cm}^{-3}$ (case 2) in steps of a factor of 10. Decreasing $c_{\mathrm{sat,org}}$ makes the condensation of organic vapour less limited by the Kelvin effect, and decreases the diameter when organic vapour starts to condense on particles. Together with the growth rate due to sulphuric acid, the minimum in total growth rate shifts to smaller particle size (see Fig. 6). When $c_{\mathrm{sat,org}}$ approaches $0\,\mathrm{cm}^{-3}$, organic vapour condenses as sulphuric acid, with a similar profile as a func-

ACPD
8, 11363–11395, 2008

tion of particle size, and the minimum in total growth rate vanishes. The simulation set showed that decreasing the saturation concentration of the condensable organic vapour lowered the correlation exponents for J_3 and N_{3-6}. With $c_{sat,org}$=0 cm^{-3} the correlation of J_3 and N_{3-6} with sulphuric acid was close to linear, the fitted exponents being n_{J3}≈1.3 and n_{N3-6}≈1.2. This is reflected by the scatter plots of Fig. 4 (case 2, d, e, f). In between these two cases (case 1 and 2), the correlation exponents for J_3 and N_{3-6} decreased gradually from n∼2–3 to n∼1, when $c_{sat,org}$ changed from 10^6 to 0 cm^{-3}.

Assuming that our simulation includes all the relevant atmospheric processes and that activation nucleation is the mechanism taking place in the atmosphere, the simulation of case 2 appears to give a closer agreement with field measurements than case 1. According to these simulations, in order to preserve the exponent n_{nuc}=1 of the nucleation rate, the growth below 3 nm must be fast and not limited by the saturation vapour concentration.

Setting $c_{sat,org}$=0 cm^{-3} for the organic vapour means that it condenses with a maximum flux and with no Kelvin effect, similarly as sulphuric acid. For sulphuric acid this assumption is reasonable, but organic substances, which are typically rather big molecules, are unlikely to be totally non-volatile. One possibility could be that some oligomeration reactions, taking place on particle surfaces, would convert semi-volatile organic vapours into particulate compounds of very low volatility (e.g. Zhang et al, 2002; Limbeck et al., 2003; Wehner et al., 2007; Heaton et al., 2007). The same growth rate profile as with $c_{sat,org}$=0 cm^{-3} could be achieved also when sulphuric acid accounts for the whole growth below ∼4 nm. However, for the conditions of Hyytiälä Boreal forest site, the sulphuric acid concentration can explain only part of the observed growth rate: Boy et al. (2005) have estimated the sulphuric acid contribution to be 4–31%. In our simulations, the sulphuric acid made 20–25% of the total growth rate (above ∼4 nm), which corresponds well to a typical situation in Hyytiälä.

3.3 Effect of the nucleated cluster size

Recently Kulmala et al. (2007) have reported experimental evidence that processes initiating atmospheric particle formation happen at particle sizes 1.5–2 nm. In the simulations presented above, activation nucleation was assumed to produce clusters of ~1 nm diameter, which has previously been thought to be the critical cluster size in atmospheric nucleation. To be concordant with recent findings, we made also simulations with nucleated cluster size of 1.5 and 2 nm.

The correlations of J_3 and N_{3-6} with sulphuric acid concentration were analysed similarly as above by making scatter plots. Time delays to sulphuric acid were determined visually by finding a value that yielded the best correlation, after which a straight line was fitted to the logarithmic data. The slope of the fitted line gives the exponent of the correlation between J_3 or N_{3-6} and sulphuric acid.

The results for the simulation cases 1 and 2, with nucleated cluster sizes 1 nm, 1.5 nm and 2 nm, are presented in Table 2. As the nucleation size gets bigger, it is obvious that the time shift between sulphuric acid and J_3 or N_{3-6} gets smaller. Also correlation exponents decrease, as aerosol dynamical processes have less time to change the relationship with sulphuric acid from that in the nucleation rate. Most importantly, with d_{nuc}=2 nm, the correlation of N_{3-6} with sulphuric acid is close to linear for both cases (case 1: n_{N3-6}=1.2, case 2: n_{N3-6}=1.0), despite the different saturation concentration for the condensable organic vapour. From Table 2 it can also be seen that $\Delta t_{J3}<\Delta t_{N3-6}$ and $n_{J3}>n_{N3-6}$, which is consistent with the analysis of measurement data (Riipinen et al., 2007) and expected as N_{3-6} is an integrated quantity of J_3.

Thus increasing the nucleated cluster size from 1 nm to 1.5–2 nm makes the correlation exponents to stay closer to the nucleation exponent, n_{nuc}=1. With d_{nuc}=1.5–2 nm we need not to reduce the saturation concentration of the condensable organic vapour ($c_{sat,org}$) greatly in order to achieve linear, or close to linear, correlation for J_3 and N_{3-6} with sulphuric acid. Already with $c_{sat,org}=10^5$ cm^{-3} the correlation exponents for J_3 and

ACPD
8, 11363–11395, 2008

N_{3-6} are in range 1–1.5. This is a promising result, since realistic values for saturation concentrations of condensable organic vapours are probably of the order 10^5–10^6 cm^{-3} (see e.g. Kulmala et al., 1998).

3.4 Activation versus ternary nucleation

As there is no definite certainty of the actual nucleation mechanism taking place in the atmosphere, we performed additional simulations with ternary H_2O-H_2SO_4-NH_3 nucleation mechanism (cases 3 and 4, for the parameters see Table 1). Ternary nucleation has been thought to be one possible mechanism for atmospheric particle formation. For an overall comparison between activation and ternary cases, see particle formation events and J_3, N_{3-6} and condensable gas concentrations in Figs. 1 and 2, respectively.

The relationships of the nucleation rate, J_3 and N_{3-6} with sulphuric acid for the ternary cases are presented in Fig. 7. The ternary nucleation rate has a steep dependence on sulphuric acid: the slope of the $\log(J_{nuc})$ vs. $\log(H_2SO_4)$ data is 5.6. This means that on average there are 5–6 H_2SO_4 molecules in the critical cluster, although the number changes slightly during the simulation according to the sulphuric acid concentration. The diameter of the critical cluster, i.e. the nucleated cluster size, is ~1 nm, as is seen from Fig. 1c and d. In ternary nucleation the critical cluster size is calculated according to theory (Napari et al., 2002), and therefore sensitivity tests with respect to cluster size are not relevant.

Similarly as with activation nucleation, the growth from nucleation size ~1 nm to 3 nm changes the relationship with sulphuric acid (Fig. 7). With ternary nucleation, the relationship of J_3 and N_{3-6} with sulphuric acid seems to vary more during the simulation: there is a bigger difference between the rising and decreasing parts of the J_3 and N_{3-6} curves than with activation nucleation (see colour code in Fig. 7). When going from J_{nuc} to J_3 and N_{3-6}, the correlation exponent decreases, as opposed to increasing exponent in cases with activation nucleation. While the nucleation exponent was n_{nuc}=5.6, the exponents for J_3 and N_{3-6} were n_{J3}=5.6 and n_{N3-6}=4.1 for case 3, and n_{J3}=5.0 and n_{N3-6}=4.0 for case 4. Also, contrary to activation nucleation cases, there is no big

ACPD
8, 11363–11395, 2008

difference in the relationship with sulphuric acid between the two ternary cases with different saturation concentration of the organic vapour. Thus it seems that in ternary cases the growth rate in 1–3 nm size range does not have such a crucial impact on the relationship between J_3 or N_{3-6} and sulphuric acid as in cases with activation nucleation. These differences between activation and ternary cases may be related to the high nucleation rates that ternary nucleation reproduces, resulting in high coagulation rates for the smallest particles, which affects the shape of the J_3 and N_{3-6} curves differently than the size-dependent growth rate.

Overall, with ternary nucleation, the correlation exponents for the relationships $J_3 \sim [H_2SO_4]^n$ and $N_{3-6} \sim [H_2SO_4]^n$ were significantly bigger than with activation mechanism. Exponents clearly exceeded unity ($n \gg 1$), and by altering any simulation parameters in reasonable ranges we were not able to reproduce correlation exponents even close to $n=2$. This illustrates that ternary H_2O-H_2SO_4-NH_3 nucleation cannot explain particle formation in atmospheric boundary layer, where observations have shown particle formation to correlate with sulphuric acid concentration to the power $n=1$–2.

4 Conclusions

The simulation results showed that the correlation with sulphuric acid can be significantly different for particle formation rate at 3 nm (J_3) and number concentration at 3–6 nm (N_{3-6}) than for nucleation rate. With activation nucleation mechanism and nucleated cluster size of 1 nm, the growth process could change the exponent from $n=1$ at the nucleation rate to $n=2.3$ for N_{3-6} and $n=3.2$ for J_3. This means, that the correlation exponents observed for J_3 or N_{3-6} should not be interpreted directly as the exponents of nucleation mechanism. In analysing the correlations between J_3 or N_{3-6} and sulphuric acid, the determination of the time shift between the quantities is of primary importance.

The main reason for the change in correlation exponent when going from J_{nuc} to J_3 and N_{3-6}, was found to be the size dependence of the growth rate between nucleation size and 3 nm. This was caused by the condensation of a semi-volatile organic vapour,

ACPD
8, 11363–11395, 2008

which gradually starts to condense on particles at size range 1–3 nm. In order to get a linear dependence on sulphuric acid for J_3 and N_{3-6}, i.e. to preserve the dependence of the nucleation rate, the saturation concentration of the organic vapour had to be decreased. With a low saturation concentration, the growth below 3 nm became faster and was not limited by the Kelvin effect anymore.

Besides the organic vapour condensation, the nucleated cluster size was observed to have a crucial effect on how the correlation with sulphuric acid appears at 3 nm particle size. Assuming activation nucleation with the nucleated cluster size of 1.5–2 nm, instead of 1 nm, reproduced correlation exponents of 1–2 for J_3 and N_{3-6}. Here the saturation concentration of organic vapour had only a minor effect. According to the present knowledge (Kulmala et al., 2007), the nucleated cluster size of 1.5–2 nm and a semi-volatile condensable organic vapour with saturation concentration of 10^5–10^6 cm^{-3} would be the most realistic parameter set. Promisingly these yielded a linear, or close to linear, relationship with sulphuric acid, consistently with the field observations.

Simulations with ternary H_2O-H_2SO_4-NH_3 nucleation yielded too steep dependence on sulphuric acid, with regard to observed exponents of 1–2 in field measurements. The correlation exponents were always greater than 4 for both J_3 and N_{3-6}, suggesting that ternary nucleation is not the valid nucleation mechanism for particle formation in atmospheric boundary layer.

It should be noted that also other aerosol dynamical processes, such as varying coagulation sink, may indirectly affect the sulphuric acid correlation during the new particle formation event. Probably those effects are of minor importance, unless the concentrations are very high, which would cause high coagulation rates.

In summary, the dependence of J_3 and N_{3-6} on sulphuric acid to the power 1–2, as observed in field measurement data, seems to require the nucleation rate to have a similar dependence on sulphuric acid with n_{nuc}=1–2. However, aerosol dynamical processes can change the correlation to some extent, and therefore correlations observed at 3 nm particle size are not necessarily the same as for nucleation rate. Thermody-

ACPD
8, 11363–11395, 2008

namic nucleation involving sulphuric acid, such as ternary nucleation, can be ruled out because it reproduces clearly incorrect dependence on sulphuric acid.

Acknowledgements. Maj and Tor Nessling foundation is acknowledged for financial support.

References

Baker, M. B. and Peter, T.: Small-scale cloud processes and climate, Nature, 451, 299–300, 2008.

Boy, M., Kulmala, M., Ruuskanen, T. M., Pihlatie, M., Reissell, A., Aalto, P. P., Keronen, P., Dal Maso, M., Hellen, H., Hakola, H., Jansson, R., Hanke, M., and Arnold, F.: Sulphuric acid closure and contribution to nucleation mode particle growth, Atmos. Chem. Phys., 5, 863–878, 2005, http://www.atmos-chem-phys.net/5/863/2005/.

Boy, M., Hellmuth, O., Korhonen, H., Nilsson, E. D., ReVelle, D., Turnipseed, A., Arnold, F., and Kulmala, M.: MALTE – model to predict new aerosol formation in the lower troposphere, Atmos. Chem. Phys., 6, 4499–4517, 2006, http://www.atmos-chem-phys.net/6/4499/2006/.

Fuchs, N. A., and Sutugin, A. G., High dispersed aerosols, in: Topics in Current Aerosol Research (Part 2), edited by G. M. Hidy and J. R. Brock, Pergamon, New York, 1–200, 1971.

Heaton, K. J., Dreyffus, M. A., Wang, S., and Johnston, M. V.: Oligomers in the early stage of biogenic secondary organic aerosol formation and growth, Environ. Sci. Technol., 41, 6129–6136, 2007.

Hirsikko, A., Laakso, L, Hõrrak, U., Aalto, P. P., Kerminen, V.-M., and Kulmala, M.: Annual and size dependent variation of growth rates and ion concentrations in boreal forest. Boreal Env. Res., 10, 357–369, 2005.

IPCC (Intergovernmental Panel on Climate Change); Climate Change 2007: The Physical Science Basis. Contribution of Working Group I to the Fourth Assessment Report of the IPCC, http://www.ipcc.ch/ipccreports/ar4-wg1.htm, 2007.

Kerminen, V.-M., Lehtinen, K. E. J., Anttila, T., and Kulmala, M.: Dynamics of atmospheric nucleation mode particles: a time scale analysis, Tellus, 56B, 135–146, 2004.

Kerminen, V.-M., Lihavainen, H., Komppula, M., Viisanen, Y., and Kulmala, M.: Direct observa-

tional evidence linking atmospheric aerosol formation and cloud droplet activation, Geophys. Res. Lett., 32, L14803, doi:10.1029/2005GL023130, 2005.
Komppula, M., Sihto, S.-L., Korhonen, H., Lihavainen, H., Kerminen, V.-M., Kulmala, M., and Viisanen, Y.: New particle formation in air mass transported between two measurement sites in Northern Finland, Atmos. Chem. Phys., 6, 2811–2824, 2006, http://www.atmos-chem-phys.net/6/2811/2006/.
Korhonen, H., Lehtinen, K. E. J., and Kulmala, M.: Multicomponent aerosol dynamics model UHMA: model development and validation, Atmos. Chem. Phys., 4, 757–771, 2004, http://www.atmos-chem-phys.net/4/757/2004/.
Korhonen, H., Kerminen, V.-M., Lehtinen, K. E. J., and Kulmala, M.: CCN activation and cloud processing in sectional aerosol models with low size resolution, Atmos. Chem. Phys., 5, 2561–2570, 2005, http://www.atmos-chem-phys.net/5/2561/2005/.
Kuang, C., McMurry, P. H., McCormick, A. V., and Eisele, F.: Dependence of nucleation rates on sulfuric acid vapor concentrations in diverse atmospheric locations, J. Geophys. Res., in press, 2008.
Kulmala, M., Toivonen, A., Mäkelä, J., and Laaksonen, A.: Analysis of the growth of nucleation mode particles observed in Boreal forest, Tellus, 50B, 449–462, 1998.
Kulmala, M., Vehkamäki, H., Petäjä, T., Dal Maso, M., Lauri, A., Kerminen, V.-M., Birmili, W., and McMurry, P. H.: Formation and growth rates of ultrafine atmospheric particles: A review of observations, J. Aerosol Sci., 35, 143–176, 2004a.
Kulmala, M., Suni, T., Lehtinen, K. E. J., Dal Maso, M., Boy, M., Reissell, A., Rannik, Ü., Aalto, P., Keronen, P., Hakola, H., Bäck, J., Hoffmann, T., Vesala, T., and Hari, P.: A new feedback mechanism linking forests, aerosols, and climate, Atmos. Chem. Phys., 4, 557–562, 2004b, http://www.atmos-chem-phys.net/4/557/2004/.
Kulmala, M., Kerminen, V. M., Anttila, T., Laaksonen, A., and O'Dowd, C. D.: Organic aerosol formation via sulphate cluster activation, J. Geophys. Res., 109, D04205, doi:10.1029/2003JD003961, 2004c.
Kulmala, M., Lehtinen, K. E. J., and Laaksonen, A.: Cluster activation theory as an explanation of the linear dependence of the formation rate of 3 nm particles and sulphuric acid concentrations, Atmos. Chem. Phys., 6, 787–793, 2006, http://www.atmos-chem-phys.net/6/787/2006/.
Kulmala, M., Riipinen, I., Sipilä, M., Manninen, H. E., Petäjä, T., Junninen, H., Dal Maso, M.,

Mordas, G., Mirme, A., Vana, M., Hirsikko, A., Laakso, L., Harrison, R. M., Hanson, I., Leung, C., Lehtinen, K. E. J., Kerminen, V.-M.: Toward Direct Measurement of Atmospheric Nucleation, Science, 318, 89–92, 2007.

Laaksonen, A., Hamed, A., Joutsensaari, J., Hiltunen, L, Cavalli, F., Junkermann, W., Asmi, A., Fuzzi, S., and Facchini, M. C.: Cloud condensation nucleus production from nucleation events at a highly polluted region, Geophys. Res. Lett., 32, L06812, doi:10.1029/2004GL022092, 2005.

Lehtinen, K. E. J. and Kulmala, M.: A model for particle formation and growth in the atmosphere with molecular resolution in size, Atmos. Chem. Phys., 3, 251–257, 2003, http://www.atmos-chem-phys.net/3/251/2003/.

Limbeck, A., Kulmala, M., and Puxbaum, H.: Secondary organic aerosol formation in the atmosphere via heterogenous reaction of gaseous isoprene on acidic particles, Geophys. Res. Lett., 30, 1996, 2003.

McMurry, P. H.: New partcle formation in the presence of an aerosol: Rates, time scales and sub-0.01 um size distributions, J. Colloid Interface Sci., 95, 72–80, 1983.

McMurry, P. H., Fink, M. A., Sakurai, H., Stolzenburg, M. R., Mauldin, L., Moore, K., Smith, J. N., Eisele, F. L., Sjostedt, S., Tanner, D., Huey, L. G., Nowak, J. B., Edgerton, E., and Voisin, D.: A criterion for new particle formation in the sulfur-rich Atlanta atmosphere, J. Geophys. Res., 110, D22S02, doi:10.1029/2005JD005901, 2005.

I. Napari, M. Noppel, H. Vehkamäki, and M. Kulmala, An improved model for ternary nucleation of sulfuric acid-ammonia-water, J. Chem. Phys. 116, 4221, 2002.

Penner, J. E., Quaas, J., Storelvmo, T., Takemura, T., Boucher, O., Guo, H., Kirkevåg, A., Kristjansson, J. E., and Seland, Ø: Model intercomparison of indirect aerosol effects, Atmos. Chem. Phys., 6, 3391–3405, 2006, http://www.atmos-chem-phys.net/6/3391/2006/.

Rannik, Ü., Aalto, P., Keronen, P., Vesala, T., and Kulmala, M.: Interpretation of aerosol particle fluxes over a pine forest: Dry deposition and random errors, J. Geophys. Res., 108(D17), 4544, 2003.

Riipinen, I., Sihto, S.-L., Kulmala, M., Arnold, F., Dal Maso, M., Birmili, W., Saarnio, K., Teinilä, K., Kerminen, V.M., Laaksonen, A., and Lehtinen, K. E. J.: Connections between atmospheric sulphuric acid and new particle formation during QUEST III–IV campaigns in Heidelberg and Hyytiälä, Atmos. Chem. Phys., 7, 1899–1914, 2007, http://www.atmos-chem-phys.net/7/1899/2007/.

Rosenfeld, D.: Aerosol, clouds, and climate, Science, 312, 1323–1324, 2006.
Sihto, S.-L., Kulmala, M., Kerminen, V.-M., Dal Maso, M., Petäjä, T., Riipinen, I., Korhonen, H., Arnold, F., Janson, R., Boy, M., Laaksonen, A., and Lehtinen, K. E. J.: Atmospheric sulphuric acid and aerosol formation: Implications from atmospheric measurements for nucleation and early growth mechanisms, Atmos. Chem. Phys., 6, 4079–4091, 2006, http://www.atmos-chem-phys.net/6/4079/2006/.
Spracklen, D. V., Carslaw, K. S., Kulmala, M., Kerminen, V.-M., Mann, G. W., and Sihto, S.-L.: The contribution of boundary layer nucleation events to total particle concentrations on regional and global scales, Atmos. Chem. Phys., 6, 5631–5648, 2006, http://www.atmos-chem-phys.net/6/5631/2006/.
Spracklen, D. V., Carslaw, K. S., Merikanto, J., Mann, G. W., Chipperfield, M. P., Kulmala, M., Sihto, S.-L., Riipinen, I., Kerminen V.-M., Lihavainen, H., Wiedensohler, A., and Birmili, W.: The contribution of particle formation to global cloud condensation nuclei concentrations, Geophys. Res. Lett., in press, 2008.
Tunved, P., Hansson, H.-C., Kerminen, V.-M., Ström, J., Dal Maso, M., Lihavainen, H., Viisanen, Y., Aalto, P. P., Komppula, M., and Kulmala, M.: High natural aerosol loading over boreal forests, Science, 312, 261–263, 2006.
Vehkamäki, H., Kulmala, M., Napari, I., Lehtinen, K. E. J., Timmreck, C., Noppel, M., and Laaksonen, A.: An improved parameterization for sulfuric acid-water nucleation rates for tropospheric can stratospheric conditions, J. Geophys. Res., 107, 4622, 2002.
Weber, R. J., Marti, J. J., McMurry, P. H., Eisele, F. L., Tanner, D. J., and Jefferson, A.: Measured atmospheric new particle formation rates: implications for nucleation mechanisms, Chem. Eng. Comm., 151, 53–64, 1996.
Weber, R. J., Marti, J. J., McMurry, P. H., Eisele, F. L., Tanner, D. J., and Jefferson A.: Measurements of new particle formation and ultrafine particle growth rates at a clean continental site, J. Geophys. Res., 102, 4375–4385, 1997.
Wehner, B., Petäjä, T., Boy, M., Engler, C., Birmili, W., Tuch, T., Wiedensohler, A., and Kulmala, M.: The contribution of sulfuric acid and non-volatile compounds on the growth of freshly formed atmospheric aerosols, Geophys. Res. Lett., 32, L17810, doi:10.1029/2005GL023827, 2005.
Zhang, K. M. and Wexler, A. S: A hypothesis for growth of fresh atmospheric nuclei, J. Geophys. Res., 107(D21), 4577, 2002.

Table 1. The simulation parameters.

	Nucleation mechanism	c_{sat} (org.) [cm^{-3}]
Case 1	Activation	10^6
Case 2	Activation	0
Case 3	Ternary	10^6
Case 4	Ternary	0

Table 2. Effect of nucleated cluster size in activation nucleation mechanism on the correlation exponents and the time delays at 3 nm (n_{J3} and Δt_{J3}: exponent and time delay for correlation of J_3 and $[H_2SO_4]$; n_{N3-6} and Δt_{N3-6}: exponent and time delay for correlation of N_{3-6} and $[H_2SO_4]$).

	d_{nuc} = 1.0 nm	d_{nuc} = 1.5 nm	d_{nuc} = 2.0 nm
Case 1 [activation, $c_{sat,org}$ = 10^6 cm^{-3}]	n_{J3} = 3.2 n_{N3-6} = 2.3 Δt_{J3} = 0.8 h Δt_{N3-6} = 1.5 h	n_{J3} = 2.2 n_{N3-6} = 1.7 Δt_{J3} = 0.5 h Δt_{N3-6} = 1.2 h	n_{J3} = 1.4 n_{N3-6} = 1.2 Δt_{J3} = 0.4 h Δt_{N3-6} = 1.0 h
Case 2 [activation, $c_{sat,org}$ = 0 cm^{-3}]	n_{J3} = 1.3 n_{N3-6} = 1.2 Δt_{J3} = 0.7 h Δt_{N3-6} = 1.2 h	n_{J3} = 1.3 n_{N3-6} = 1.1 Δt_{J3} = 0.5 h Δt_{N3-6} = 1.1 h	n_{J3} = 1.1 n_{N3-6} = 1.0 Δt_{J3} = 0.3 h Δt_{N3-6} = 0.8 h

ACPD
8, 11363–11395, 2008

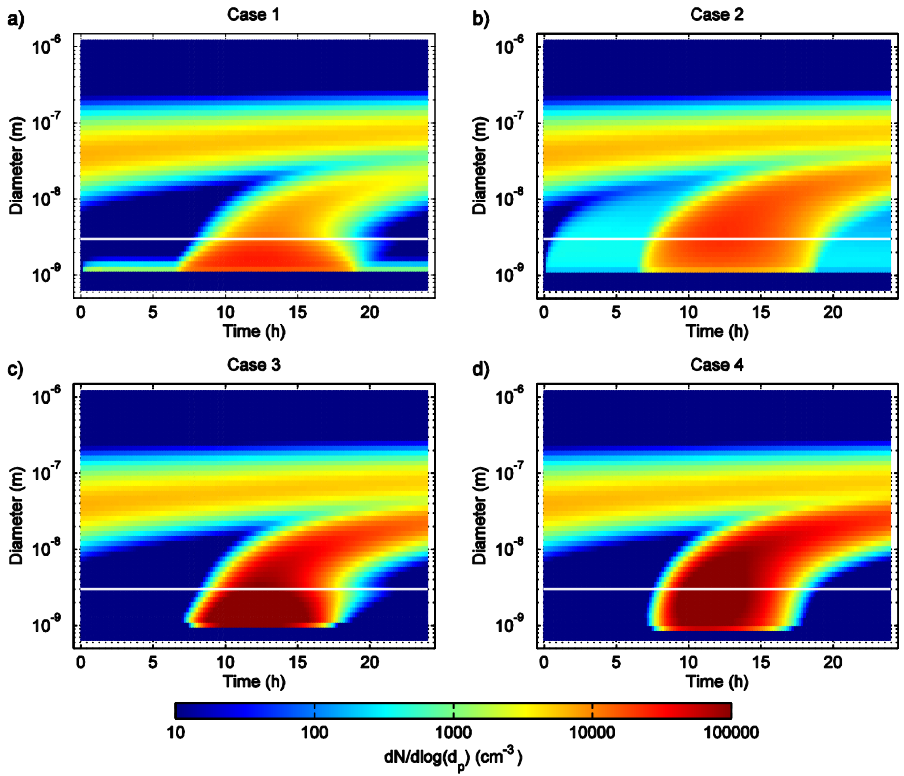

Fig. 1. Simulated new particle formation event for cases 1–4. **(a)** Case 1: activation nucleation, $c_{sat,org}$=10^6 cm^3, **(b)** Case 2: activation nucleation, $c_{sat,org}$=0 cm^3, **(c)** Case 3: ternary nucleation, $c_{sat,org}$=10^6 cm^3 **(d)** Case 4: ternary nucleation, $c_{sat,org}$=0 cm^3. Particle diameter is on y-axis, simulation time on x-axis and colour indicates the normalised number concentration. White horizontal line shows the 3 nm border, which is the typical lower limit for particle size distribution measurements.

ACPD
8, 11363–11395, 2008

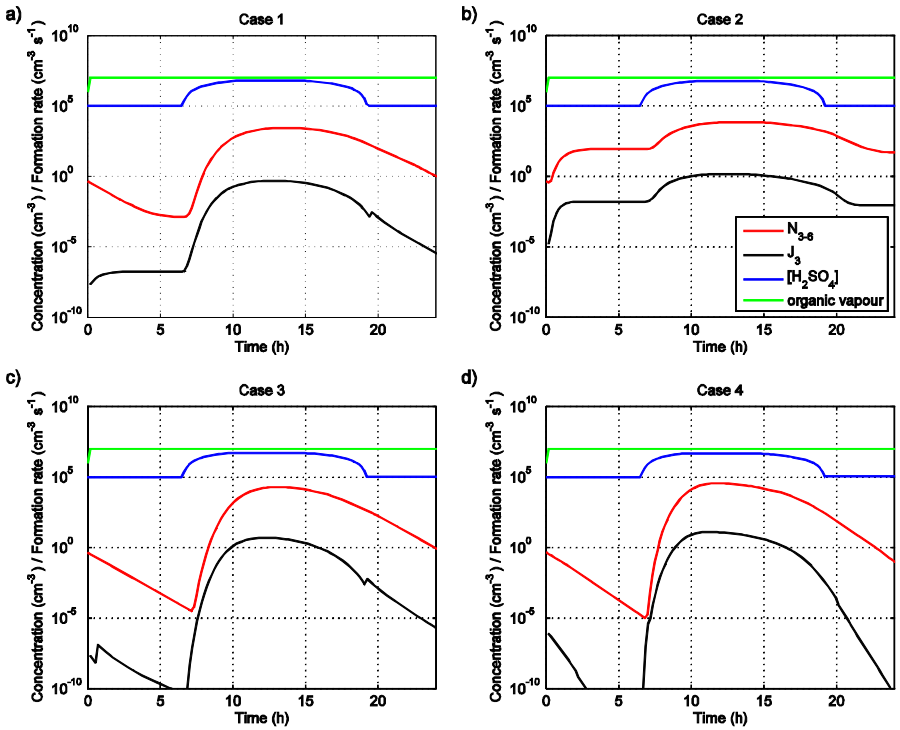

Fig. 2. Condensable gas concentrations (sulphuric acid and an organic vapour, given as input for the simulation) and simulated formation rate of 3 nm particles (J_3) and number concentration of 3–6 nm particles (N_{3-6}) as a function of time for simulation cases 1–4 (a–d).

ACPD
8, 11363–11395, 2008

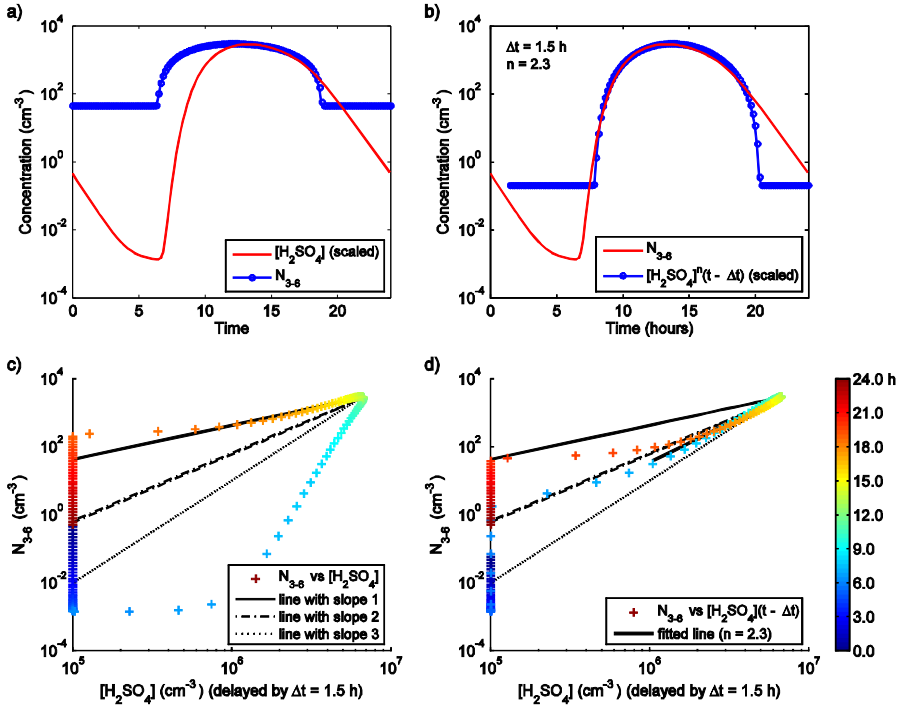

Fig. 3. The effect of time delay on the correlation between sulphuric acid concentration ([H_2SO_4]) and number concentration of 3–6 nm particles (N_{3-6}) (case 1). a) N_{3-6} and [H_2SO_4] as a function of time during the simulation. b) [H_2SO_4] delayed by a time shift Δt=1.5 h and raised to exponent n=2.3, corresponding the best correlation. c) $N_{3-6}(t)$ versus [H_2SO_4](t) without time shift. d) $N_{3-6}(t)$ versus [H_2SO_4]($t-\Delta t$), i.e. [H_2SO_4] values delayed by Δt=1.5 h. The time of day (t=0...24 h) is indicated by colour code.

ACPD
8, 11363–11395, 2008

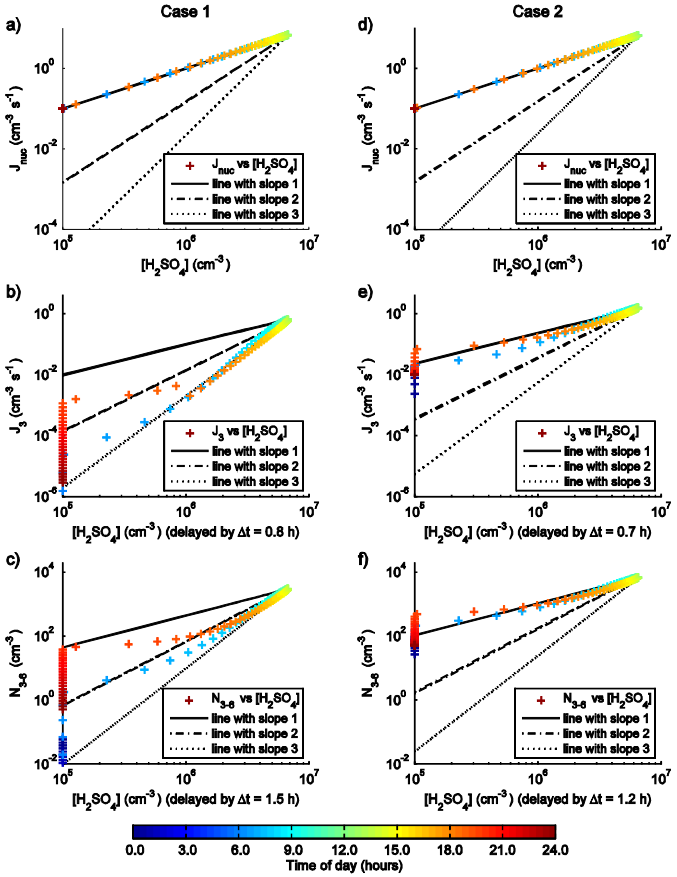

Fig. 4. Correlation of nucleation rate (J_{nuc}, top), 3 nm particle formation rate (J_3, middle) and 3-6 nm particle number concentration (N_{3-6}, bottom) with $[H_2SO_4]$ for simulation cases 1 (a, b, c) and 2 (d, e, f) with activation as nucleation mechanism. For J_3 and N_{3-6} scatter plots $[H_2SO_4]$ has been delayed by the time shift Δt determined visually from the data to give the best correlation. Straight lines with slopes 1, 2 and 3 correspond the exponential dependences $\sim[H_2SO_4]$, $\sim[H_2SO_4]^2$, $\sim[H_2SO_4]^3$. The time of day (t=0...24 h) is indicated by colour code.

ACPD
8, 11363–11395, 2008

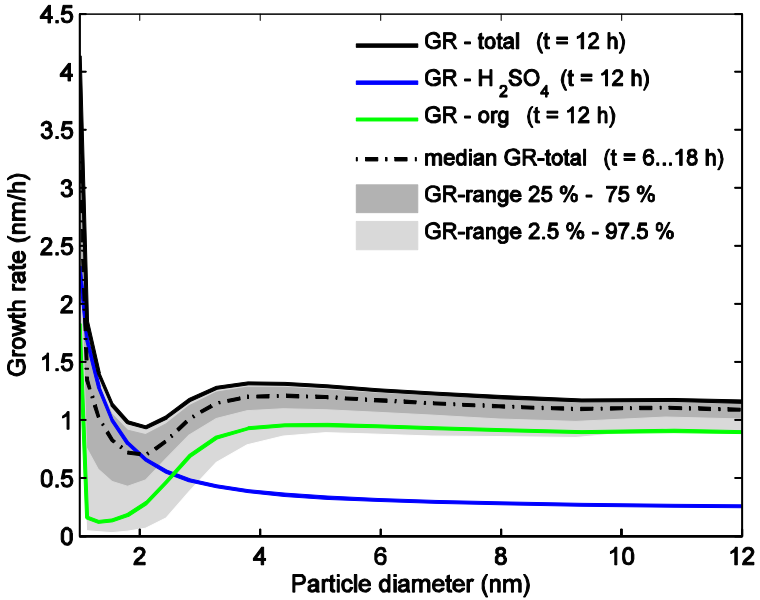

Fig. 5. Particle growth rate as a function of particle size for simulation case 1. Solid lines show the growth rate at noon (t=12 h), with the contributions of sulphuric acid (blue) and organic vapour (green) separated. Grey areas indicate the 25 and 2.5 percentiles showing the growth rate variability during the event time (from 6 a.m. to 6 p.m., t=6...18 h).

ACPD
8, 11363–11395, 2008

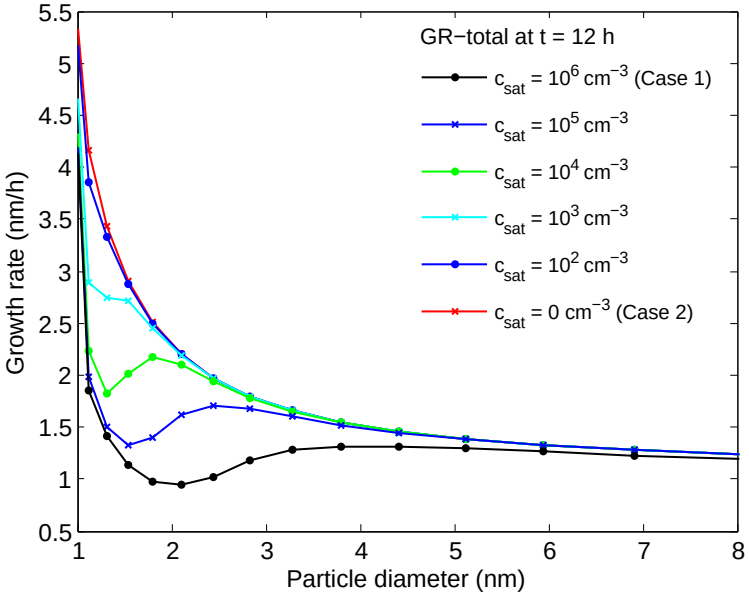

Fig. 6. Particle growth rate (total=H_2SO_4+organic) at noon (t=12 h) as a function of particle size with different saturation concentration (c_{sat}) values for the condensable organic vapour.

ACPD
8, 11363–11395, 2008

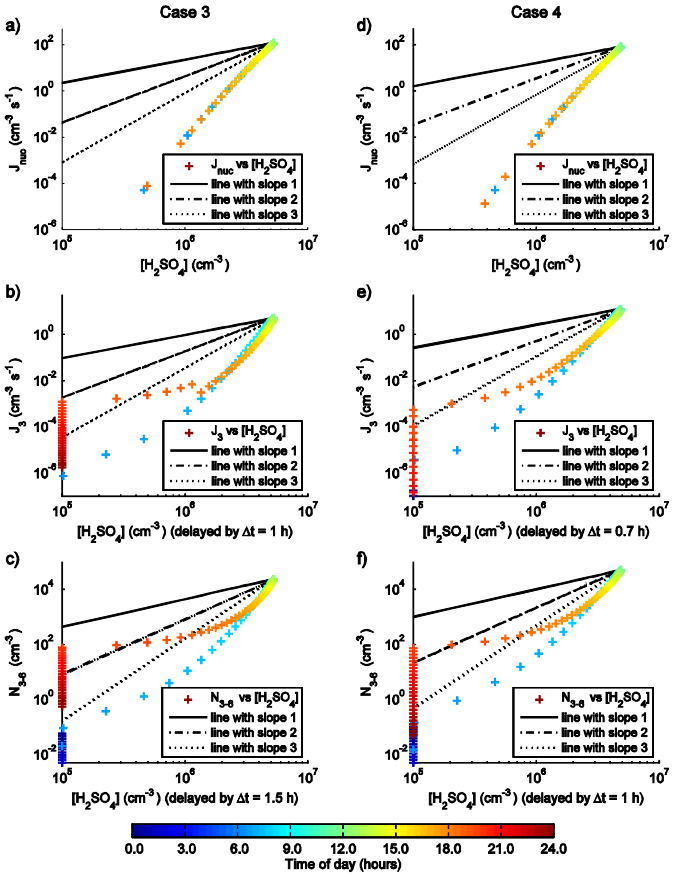

Fig. 7. Correlation of nucleation rate (J_{nuc}, top), 3 nm particle formation rate (J_3, middle) and 3–6 nm particle number concentration (N_{3-6}, bottom) with $[H_2SO_4]$ for simulation cases 3 (a, b, c) and 4 (d, e, f) with ternary nucleation. See Fig. 4 for more explanations.

ACPD
8, 11363–11395, 2008